HHS Public Access

Author manuscript

Cell Rep. Author manuscript; available in PMC 2019 January 18.

Published in final edited form as:

Cell Rep. 2019 January 08; 26(2): 322–329.e3. doi:10.1016/j.celrep.2018.12.049.

Reduced SERCA Function Preferentially Affects Wnt Signaling by Retaining E-Cadherin in the Endoplasmic Reticulum

Annabelle Suisse[1] and **Jessica E. Treisman**[1,2,*]

[1]Kimmel Center for Biology and Medicine at the Skirball Institute and Department of Cell Biology, NYU School of Medicine, 540 First Avenue, New York, NY 10016, USA

[2]Lead Contact

SUMMARY

Calcium homeostasis in the lumen of the endoplasmic reticulum is required for correct processing and trafficking of transmembrane proteins, and defects in protein trafficking can impinge on cell signaling pathways. We show here that mutations in the endoplasmic reticulum calcium pump SERCA disrupt Wingless signaling by sequestering Armadillo/β-catenin away from the signaling pool. Armadillo remains bound to E-cadherin, which is retained in the endoplasmic reticulum when calcium levels there are reduced. Using hypomorphic and null *SERCA* alleles in combination with the loss of the plasma membrane calcium channel Orai allowed us to define three distinct thresholds of endoplasmic reticulum calcium. Wingless signaling is sensitive to even a small reduction, while Notch and Hippo signaling are disrupted at intermediate levels, and elimination of SERCA function results in apoptosis. These differential and opposing effects on three oncogenic signaling pathways may complicate the use of SERCA inhibitors as cancer therapeutics.

In Brief

Suisse and Treisman describe genetic conditions that reduce calcium in the endoplasmic reticulum to three distinct extents. They find that Wnt signaling is more sensitive to changes in calcium levels than the Notch and Hippo pathways, potentially complicating the use of calcium pump inhibitors as cancer therapeutics.

Graphical Abstract

*Correspondence: jessica.treisman@nyulangone.org.

AUTHOR CONTRIBUTIONS

A.S. and J.E.T. conceived and designed the experiments, performed the experiments, analyzed the data, and wrote the manuscript.

SUPPLEMENTAL INFORMATION

Supplemental Information includes four figures and one table and can be found with this article online at https://doi.org/10.10167j.celrep.2018.12.049.

DECLARATION OF INTERESTS

The authors declare no competing interests.

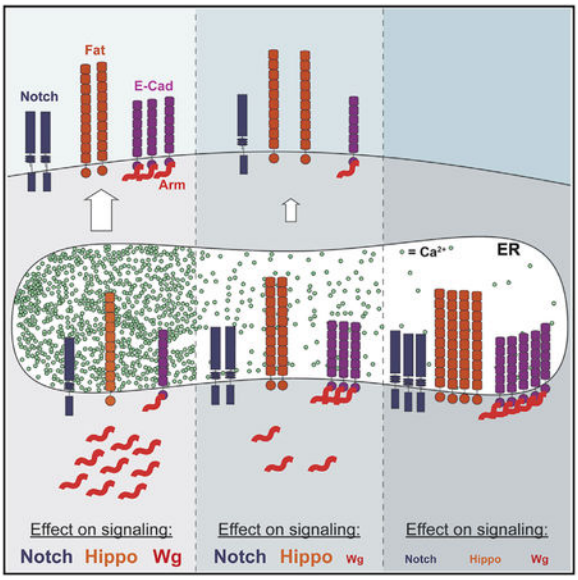

INTRODUCTION

Transmembrane proteins must pass through the secretory pathway to reach the cell surface, where they can interact with other cells and respond to signaling cues. Disrupting the environment in the first secretory compartment, the endoplasmic reticulum (ER), causes misfolding of transmembrane and secreted proteins and elicits a stress response that can either restore proteostasis or trigger apoptosis (Walter and Ron, 2011). The ER acts as a store of intracellular calcium (Ca^{2+}) that can be rapidly released into the cytoplasm to trigger a variety of cellular responses (Bagur and Hajnoczky, 2017). The sarcoplasmic-ER ATPase (SERCA) actively pumps Ca^{2+} into the ER, increasing its concentration to 1,000-fold higher than in the cytosol (Wuy- tack et al., 2002). Depletion of Ca^{2+} from the ER is sensed by Stim, which accumulates at ER-plasma membrane junctions and activates Orai, a Ca^{2+} channel in the plasma membrane that mediates store-operated calcium entry (SOCE) (Prakriya and Lewis, 2015). SERCA colocalizes with Stim-Orai complexes, allowing entering Ca^{2+} to be pumped directly into the ER (Alonso et al., 2012). SOCE maintains Ca^{2+} homeostasis in the ER so that Ca^{2+}-binding proteins can fold correctly. In the absence of SERCA, the cell-surface receptor Notch, which has extracellular EGF and Lin-12/Notch repeats that interact with Ca^{2+}, fails to mature (Periz and Fortini, 1999; Roti et al., 2013).

Wnt signaling relies on the bifunctional β-catenin protein, which acts as an essential linker between E-cadherin (E-Cad) and α-catenin at adherens junctions (AJs), but also enters the nucleus and regulates target gene expression in cells that receive a Wnt signal (Brembeck et al., 2006). In the absence of Wnt, cytoplasmic β-catenin is phosphorylated within a destruction complex, leading to its ubiquitination and degradation (Stamos and Weis, 2013). Junctional β-catenin is distinct from the pool available for Wnt signaling, and excess E-Cad can remove β-catenin from the signaling pool (Sanson et al., 1996). The extracellular domain of E-Cad binds Ca^{2+} ions at the junctions between cadherin domains, giving it a rigid structure (Courjean et al., 2008). The cadherin family also includes the large

protocadherins Fat and Dachsous, which restrict growth by activating the Hippo signaling pathway and regulate planar cell polarity (Sadeqzadeh et al., 2014; Sharma and McNeill, 2013). The precise conformation of these molecules depends on Ca^{2+} binding by only a subset of their cadherin domain linkers (Tsukasaki et al., 2014).

There has been significant interest in using SERCA inhibitors such as thapsigargin as cancer therapeutics due to their ability to induce ER stress and apoptosis (Cui et al., 2017). Their general toxicity means that they would need to be targeted to specific cancer cell types (Denmeade et al., 2012). However, activating mutations in Notch that are found in certain types of leukemia may make this receptor especially sensitive to reduced SERCA function (Roti et al., 2013). Here, we show that a hypomorphic mutation in *Drosophila SERCA* preferentially affects signaling by the Wnt Wingless (Wg), because E-Cad is retained in the ER and sequesters bound Armadillo (Arm)/β-catenin. Complete loss of *SERCA* function leads to apoptosis, but an intermediate reduction in ER Ca^{2+} induced by mutating *orai* in the hypomorphic *SERCA* background disrupts Hippo signaling, leading to overgrowth and Notch signaling. These results imply that Wnt-driven cancers may be the most sensitive to SERCA inhibition but highlight the risk that inhibitors may activate cell proliferation through the Hippo pathway.

RESULTS

Arm Accumulates in an Inactive State in the Absence of SERCA

In a mosaic genetic screen (Janody et al., 2004), we isolated a recessive lethal mutation that had a paradoxical effect on Wg signaling. Clones of mutant cells in the larval wing imaginal disc showed accumulation of Arm but reduced expression of *aristaless* (*al*) (Figure 1B), which is a Wg target gene (Figures 1D and S1A). The expression of several other Wg target genes, *Distal-less* (*Dll*), *vestigial* (*vg*), and the reporter *frizzled3-RFP (fz3-RFP)* (Neumann and Cohen, 1997; Olson etal., 2011; Zecca et al., 1996), was likewise reduced in mutant clones in the wing disc (Figures S1C, S1E, and S1F). However, *achaete* (*ac*) and *senseless* (*sens*), which are expressed in sensory organ precursors at the wing margin in response to Wg signaling, were not affected (Figures S1G and S1H). Since Arm was present but showed reduced transcriptional activity, we named our mutant allele *disarmed* (*dsm*). We mapped *dsm* to the gene *sarco-endo-plasmic reticulum* Ca^{2+}*-ATPase (SERCA)* and found that it changes Gly148 to Asp (Figure 1A). The *dsm* mutation is within the activation domain of the SERCA pump (Lee and East, 2001) and may affect the coupling of Ca^{2+} transport to ATP hydrolysis. $SERCA^{dsm}$ did not complement two other *SERCA* alleles, $SERCA^{Kum170}$ (Glu442 to Lys) (Sanyal et al., 2005) and $SERCA^{S5}$ (Periz and Fortini, 1999), which we found to be a nonsense mutation at Gln108 (Figure 1A). These mutations also caused Arm accumulation and loss of Wg target gene expression (Figures 1C, S1B, and S1D). Furthermore, the $SERCA^{S5}$ phenotype was fully rescued by expressing *UAS- SERCA* within the mutant clones (Figure S1I), confirming that the effect on Wg signaling is due to the loss of SERCA function.

To determine where in the Wg pathway SERCA acts to prevent Arm accumulation, we made clones mutant for both *SERCA* and *arrow* (*arr*), which encodes the Wg co-receptor (Wehrli et al., 2000). In *arr* mutant clones, *al* expression was lost and Arm was not increased (Figure

1D). Like *SERCA*^{S5} clones (Figure 1C), *arr*^{63D} *SERCA*^{S5} double mutant clones lost *al* expression but accumulated Arm (Figure 1E). This indicates that the accumulation of non-functional Arm in the absence of *SERCA* does not require Wg pathway activity. Moreover, the Arm that accumulated in *SERCA* clones was not phosphorylated, unlike the Arm present in clones lacking the ubiquitin ligase subunit Cullin1, suggesting that the loss of SERCA blocks Arm degradation by preventing its phosphorylation by the destruction complex (Figures 1F and 1G).

Loss of SERCA Results in Arm Sequestration by E-Cad Retained in the ER

In addition to its role as a transcription factor for Wg target genes, Arm links E-Cad at AJs to α-catenin and thus to the actin cyto-skeleton (Brembeck et al., 2006). In *SERCA* mutant clones, we found that E-Cad accumulated together with Arm basal to the normal AJ location (Figures 2A, 2B, and S2A). To identify the compartment in which E-Cad and Arm accumulated, we used the inhibitor thapsigargin (Tg) (Thastrup et al., 1990) to block SERCA function in S2 cells transfected with E-Cad. In control cells, E-Cad and Arm were present at the plasma membrane, labeled with phalloidin to detect cortical actin (Figures 2C and 2D). Tg treatment resulted in the loss of E-Cad and Arm from the cell surface; instead, these proteins colocalized with the ER marker Calnexin99A (Cnx99A) (Riedel et al., 2016) (Figures 2E–2G), suggesting that they are trapped at the ER membrane.

To test whether Arm was sequestered on the ER by binding to E-Cad, we knocked down *E-Cad* by RNAi in *SERCA* mutant clones. This prevented Arm accumulation, but some reduction in *al* expression was still observed, potentially due to poor cell viability in the absence of E-Cad (Figures 2H and 2I). To specifically prevent *E*-Cad from binding to Arm without affecting the health ofthe cells, we used knockin alleles of *E-Cad* that remove a cluster of serines or a larger region required for Arm binding but fuse the cytoplasmic domain directly to α-catenin, allowing it to function normally at AJs (*E-Cad*$^{\Delta S\text{-}\alpha Cat}$ and *E-Cad*$^{\Delta\beta S\text{-}\alpha Cat}$) (Chen et al., 2017). In *E-Cad*$^{\Delta S\text{-}\alpha Cat}$ and *E-Cad*$^{\Delta\beta S\text{-}\alpha Cat}$ clones, membrane-bound Arm was lost and *al* was unaffected, showing that releasing Arm from AJs made it less stable and did not increase Wg signaling (Figures 2J and S2E). Normal *al* expression was restored in *SERCA, E-Cad*$^{\Delta S\text{-}\alpha Cat}$ and *SERCA, E-Cad*$^{\Delta\beta S\text{-}\alpha Cat}$ double mutant clones, which also showed reduced Arm levels, confirming that accumulation and inactivation of Arm in *SERCA* mutant cells depends on its binding to E-Cad (Figures 2K and S2F). These results suggest that the loss of SERCA disrupts E-Cad trafficking to the plasma membrane, resulting in the mislocalization of Arm bound to the cytoplasmic domain of E-Cad.

Wg Signaling Is Highly Sensitive to Reduced ER Ca^{2+} Levels

In *SERCA* mutant cells, Arm recruitment to E-Cad at the ER could result from either lower Ca^{2+} levels in this compartment or increased levels in the cytoplasm, although SERCA inhibition has only a small effect on cytosolic Ca^{2+} (Sehgal et al., 2017). To test the second possibility, we reduced Ca^{2+} levels in the cytosol in *SERCA* mutant cells by preventing SOCE. Cells doubly mutant for the null *SERCA*^{S5} allele and *orai*, which encodes the plasma membrane Ca^{2+} channel (Prakriya et al., 2006; Venkiteswaran and Hasan, 2009), still accumulated Arm and lost *al* expression, indicating that the sequestration of Arm by E-Cad is not due to increased cytoplasmic Ca^{2+} (Figure 3B). This result was confirmed by

knocking down the ER Ca^{2+} sensor Stim in *SERCA*^{S5} mutant cells (Figures S3A–S3C), using an RNAi line that has been shown to affect Stim expression and function (Eid et al., 2008).

SERCA^{dsm}, *orai*^{k11505} double mutant clones showed a stronger reduction of *al* and accumulation of Arm than *SERCA*^{dsm} single mutant clones (Figure 3C). If *SERCA*^{dsm} retains some function, then disabling SOCE in *SERCA*^{dsm} mutant cells would further decrease ER Ca^{2+}. Since changes in luminal Ca^{2+} concentration are known to trigger the unfolded protein response (UPR) (Zhang and Kaufman, 2006), we assessed ER stress as an indirect measure of ER Ca^{2+} by using a reporter that expresses GFP only when *Xbp1* is spliced by the stress sensor Ire1 (Ryoo et al., 2007). The quantification of GFP expression in mutant clones revealed three distinct levels of ER stress (Figures 3D–3G). *SERCA*^{dsm} only weakly induced ER stress, while *SERCA*^{S5} produced the strongest response. *SERCA*^{dsm}, *orat*^{11505} double mutant cells expressed an intermediate amount of GFP, indicating that preventing Ca^{2+} entry into *SERCA*^{dsm} cells further reduced ER Ca^{2+} levels. The strong ER stress in *SERCA*^{S5} mutant cells resulted in cell death, as shown by the activation of caspase 3 (Figure 3F”). These data show that even a small reduction in ER Ca^{2+} that causes low levels of stress without affecting cell survival is sufficient to affect E-Cad trafficking and Wg signaling. The effect on E-Cad is quite specific, as the slight ER Ca^{2+} reduction in *SERCA*^{dsm} mutants did not cause ER retention of several other transmembrane proteins (Figures S3D–S3F).

The Wg, Hippo, and Notch Pathways Are Differentially Sensitive to ER Ca^{2+}

SERCA^{dsm}, *orai*^{k11505} double mutant clones were generally larger than clones that are homozygous for either single mutation and had a rounded shape with smooth borders (Figures 3C and 3E), resembling *fat* mutant clones, in which the Hippo pathway is disabled (Willecke et al., 2006; Silva et al., 2006; Bennett and Harvey, 2006). Fat is a protocadherin with 12 Ca^{2+}-binding domains. We assessed the effect of the three genotypes on Fat trafficking and on Dachs, a myosin that accumulates at the plasma membrane when Fat signaling is reduced (Mao et al., 2006). We found that *SERCA*^{dsm} had little effect on Fat or Dachs (Figures 4A, 4D, and S4A). In *SERCA*^{dsm}, *orai*^{k11505} double mutant clones and *SERCA*^{S5} clones, Fat strongly accumulated in subapical regions and was lost from the apical plasma membrane (Figures 4B, 4C, S4B, and S4C). High levels of Dachs were present at the membrane in these clones, indicating a loss of Fat activity (Figures 4E and 4F). However, only *SERCA*^{dsm}, *orai*^{k11505} clones showed increased growth, since *SERCA*^{S5} mutant cells undergo apoptosis (Figure 3G”). Crumbs (Crb), another transmembrane protein that regulates Hippo signaling (Chen et al., 2010; Ling et al., 2010; Robinson et al., 2010), did not show clear changes in its localization in *SERCA*^{dsm}, *orai*^{k11505} double mutant clones or *SERCA*^{S5} clones (Figure S4D).

SERCA mutations also affect Notch signaling by impairing Notch cleavage and trafficking to the cell surface (Periz and For- tini, 1999). Moderate levels of Notch accumulated in subapical puncta in *SERCA*^{dsm} clones without affecting the expression of its target gene Cut (Figures 4G and 4J). *SERCA*^{dsm}, *orai*^{k11505} double mutant clones and *SERCA*^{S5} clones showed more Notch accumulation and failed to activate Cut (Figures 4H, 4I, 4K, and 4L).

The three distinct ER Ca^{2+} levels thus produce different outcomes; Wg signaling is the most sensitive and apoptosis the least sensitive to reductions in ER Ca^{2+}, while at intermediate levels, Notch signaling and Hippo signaling are reduced.

DISCUSSION

Our characterization of a hypomorphic *SERCA* mutant allele revealed that E-Cad trafficking is especially sensitive to reduced ER Ca^{2+} levels and that retention of E-Cad in the ER under these mild stress conditions sequesters Arm away from the pool available for Wg signaling. A similar ER retention of E-Cad and desmosomal cadherins, leading to the loss of cell adhesion, has been demonstrated in human keratinocytes in Darier disease, which results from a mutation in *SERCA2* (Savignac et al., 2014). In addition, ER stress promotes the differentiation of mouse intestinal stem cells (Heijmanset al., 2013), suggesting that this may be a physiological mechanism to reduce the Wnt signaling that is required for stem cell maintenance (Krausova and Korinek, 2014). Ca^{2+} is essential for the homophilic binding of cadherin extracellular domains that mediates cell adhesion (Koch et al., 1997; Vendome et al., 2011). Cadherin monomers contain multiple cadherin domains separated by hinge regions that can each bind three Ca^{2+} ions, stabilizing the molecule to form a rod-like structure that is resistant to protease cleavage (Boggon et al., 2002; Courjean et al., 2008). In larger cadherins, some of the linker regions are Ca^{2+} free and remain flexible (Jin et al., 2012; Tsukasaki et al., 2014). Cadherin folding into the correct conformation may thus be very sensitive to Ca^{2+} levels in the ER. In mammalian cells, Tg-induced ER stress leads to O-GlcNAc glycosylation of the E-Cad cytoplasmic domain, blocking its exit from the ER (Zhu et al., 2001). However, this modification depends on caspase induction by ER stress-induced apoptosis (Zhu et al., 2001), which does not occur in $SERCA^{dsm}$ mutant clones. It is also possible that E-Cad is not affected by ER Ca^{2+} levels directly, but is especially sensitive to the general reduction in secretion caused by the loss of SERCA (Ke et al., 2018).

Arm that is bound to E-Cad at the ER membrane appears to be unavailable for Wg signaling. In mammalian cells, β-catenin forms a complex with E-Cad during co-translation in the ER and helps to transport E-Cad from the ER to the Golgi (Chen et al., 1999; Curtis et al., 2008). Depleting ER Ca^{2+} levels may enhance the binding of Arm to E-Cad at the ER, as low extracellular Ca^{2+} induces rapid Arm recruitment to E-Cad at the plasma membrane (Kim et al., 2011). Because E-Cad competes with adenomatous polyposis coli and Axin to bind to the Arm domains, a stronger Arm-E-Cad interaction could both protect Arm from degradation and prevent it from translocating into the nuclei of Wg-receiving cells (Sanson et al., 1996). The mechanism by which β-catenin enters the nucleus is poorly understood (Griffin et al., 2018), and it is possible that mislocalization at the ER membrane would exclude it from docking with the partner proteins required for nuclear import.

Using two *SERCA* alleles and a *SERCA orai* mutant combination, we were able to produce three distinct levels of ER Ca^{2+} that revealed the differential sensitivities of three oncogenic pathways. Wg signaling is the most sensitive, as it is disturbed by the weak allele $SERCA^{dsm}$; while Notch trafficking is also abnormal in this mutant background, Notch target genes can still be activated. Afurther reduction in ER Ca^{2+} produced by disrupting SOCE prevents Notch and Hippo signaling, probably through effects on the trafficking of

Notch (Periz and Fortini, 1999) and the large protocadherin Fat, but only complete loss of *SERCA* induces apoptosis. These findings have important implications for the use of SERCA inhibitors such as Tg as cancer therapeutics, even when targeted to specific cell types (Denmeade et al., 2012; Roti et al., 2013). Although it may be possible to selectively block Wnt-driven cancers with low doses of such inhibitors, the level of inhibition needed to prevent Notch signaling is likely to actually enhance tumor invasiveness by downregulating FAT family members and thus disrupting Hippo signaling (Katoh, 2012; Yu etal., 2015).

STAR⋆METHODS

CONTACT FOR REAGENT AND RESOURCE SHARING

Further information and requests for resources and reagents should be directed to and will be fulfilled by the Lead Contact, Jessica Treisman (jessica.treisman@nyulangone.org).

EXPERIMENTAL MODEL AND SUBJECT DETAILS

Drosophila melanogaster strains were maintained on cornmeal/agar molasses fly food at room temperature (20°C). Third instar larvae of both sexes were used for all wing imaginal disc stainings. $SERCA^{dsm}$, $SERCA^{S5}$ (Perizand Fortini, 1999) and $SERCA^{kum170}$ (Sanyal et al., 2005) were recombined with FRT42D and with $orai^{k11505}$ (Venkiteswaran and Hasan, 2009), arr^{63D} (Janody et al., 2004), *fz3-RFP* (Olson et al., 2011) or the knock-in alleles *E-Cad*$^{\Delta S\text{-}\alpha Cat}$*-GFP* or *E-Cad*$^{\Delta\beta S\text{-}\alpha Cat}$*-GFP* (Chen et al., 2017), or combined with *UAS-Xbp1-GFP* (Ryoo et al., 2007), *UAS-E-Cad RNAi* (HMS00693) or *UAS-Stim.RNAi.E* (Eid et al., 2008) on the third chromosome. Other stocks used were *FRT42,* $cul1^{Ex}$ (Ou et al., 2002) and *FRT82,* axn^{E77} (Lee and Treisman, 2001). Homozygous clones were generated by crossing to *Ubx-FLP, UAS-CD8-GFP; FRT42, tub-GAL80/Cy0; tub-GAL4/TM6B* or *Ubx-FLP; FRT42, ubi-RFP* or *Ubx-FLP; FRT42, ubi-GFP* or *Ubx-FLP; FRT42, ubi-RFP/CyO; hh-GAL4/TM6B* or *Ubx-FLP; FRT82, ubi-RFP*. Genotypes for all panels are given in Table S1. S2 cells were maintained at 25°C in Schneider's medium supplemented with 10% fetal calf serum. We believe this cell line to be male based on unpublished RNA-Seq experiments in which we detected expression of a gene on the Y chromosome.

METHOD DETAILS

Identification of SERCA^{dsm} mutation—The *dsm* mutation was identified in the screen described in (Janody et al., 2004). The lethality of the mutation was mapped by complementation tests with deficiencies on the same chromosome arm, and localized between the cytological bands 60A9 and 60A13 by failure to complement *Df(2R)BSC601* and complementation of *Df(2R)BSC770*. Sequencing of genes within this region from homozygous *dsm* embryos revealed the G148D mutation in *SERCA*.

Immunohistochemistry—Wing discs were dissected in 0.1M sodium phosphate buffer pH 7.2 and fixed for 30 min on ice in 4% formaldehyde in PEM (0.1 M PIPES pH 7.0, 2mM $MgSO_4$,1mM EGTA). Discs were washed for 15 min on ice in 0.1M sodium phosphate buffer pH7.2/0.2% Triton X-100, and incubated overnight in primary antibodies in 0.1M sodium phosphate buffer pH7.2/0.2% Triton X-100/10% normal donkey serum (Jackson Immunoresearch). After three 5 min washes at room temperature in 0.1M phosphate buffer

pH7.2/0.2% Triton X-100, they were incubated in secondary antibodies for 2–4 h at 4°C in 0.1M sodium phosphate buffer pH7.2/0.2% Triton X-100/10% normal donkey serum, and washed as above before mounting in 80% glycerol in phosphate-buffered saline pH 7.0. Antibodies used were rat anti-Al (1:1000) (Campbell et al., 1993), chicken anti-GFP (1:300; Invitrogen), mouse anti-Arm (1:10; Developmental Studies Hybridoma Bank (DSHB)), rabbit anti-phospho-β-catenin (1:20; Cell Signaling #9564), rat anti-E-Cad (1:20; DSHB), rabbit anti-active Caspase3 (1:500; BD PharMingen), mouse anti-Notch (1:10; DSHB), mouse anti-Cut (1:10; DSHB), mouse anti-Cnx99a (1:10; DSHB), mouse anti-Achaete (1:10; DSHB), mouse anti-Fz2 (1:10; DSHB), mouse anti-Crb (1:10; DSHB), rabbit anti-Fat (1:1,000) and rat anti-Dachs (1:1,000) (Brittle et al., 2012), rat anti-Dll (1:500) (Uhl et al., 2016), rabbit anti- Vg (1:200) (Williams et al., 1991), guinea pig anti-Sens (1:1000) (Nolo et al., 2000), rabbit anti-EGFR (1:500) (Rodrigues et al., 2005), rabbit anti-Hbs (1:400) (Linneweber et al., 2015), and Alexa Fluor 555-conjugated Phalloidin (Invitrogen). Fluorescent secondary antibodies (1:200) were from Jackson Immunoresearch, and images were obtained using a Leica SP5 confocal microscope.

Cell culture—To look at ECad and Arm protein localization, 10^6 cells/well were transfected with 300 ng *pAct5c-Gal4* and 300 ng *pUAS-E-Cad* (Sarpal et al., 2012) using Effectene Transfection Reagent (QIAGEN, Germantown, USA). On day 2, the cells were supplemented with 10 μM Tg to block SERCA activity. On day 5, the cells were collected for immunohistochemistry in chamber slides and stained as described above for imaginal discs.

QUANTIFICATION AND STATISTICAL ANALYSIS

Quantification of GFP signal intensity was performed using ImageJ by measuring average signal intensity in RFP negative clones in the posterior compartment, after subtracting the background in adjacent RFP positive regions of the same size. Significance was evaluated by Welch's ANOVA due to unequal variances between the samples. All panels show images representative of at least 10 discs examined.

For cell staining quantifications, three independent cell treatments were performed and between 45 and 150 cells were counted per sample. E-Cad was considered to be at the plasma membrane when it colocalized with the phalloidin signal. Significance was evaluated by unpaired t test. We determined that the variances of the two conditions were not significantly different.

Supplementary Material

Refer to Web version on PubMed Central for supplementary material.

ACKNOWLEDGMENTS

We thank Hugo Bellen, Gerard Campbell, Sean Carroll, Cheng-Ting Chien, Karl Fischbach, Mark Fortini, Brian Gebelein, Yang Hong, Andrea Page- McCaw, Aloma Rodrigues, Hyung Don Ryoo, David Strutt, Ulrich Tepass, the Bloomington *Drosophila* Stock Center, and the Developmental Studies Hybridoma Bank for fly stocks and reagents. We are grateful to DanQing He for technical assistance and advice. The manuscript was improved by the critical comments of Carolyn Morrison, Josefa Steinhauer, and Hongsu Wang. This work was supported by the NIH (grant EY13777 to J.E.T.).

REFERENCES

Alonso MT, Manjarrés IM, and García-Sancho J (2012). Privileged coupling between Ca($^{2+}$) entry through plasma membrane store-operated Ca($^{2+}$) channels and the endoplasmic reticulum Ca($^{2+}$) pump. Mol. Cell. Endocrinol 353, 37–44. [PubMed: 21878366]

Bagur R, and Hajnoczky G (2017). Intracellular Ca^{2+} sensing: its role in calcium homeostasis and signaling. Mol. Cell 66, 780–788. [PubMed: 28622523]

Bennett FC, and Harvey KF (2006). Fat cadherin modulates organ size in *Drosophila* via the Salvador/Warts/Hippo signaling pathway. Curr. Biol 16, 2101–2110. [PubMed: 17045801]

Boggon TJ, Murray J, Chappuis-Flament S, Wong E, Gumbiner BM, and Shapiro L (2002). C-cadherin ectodomain structure and implications for cell adhesion mechanisms. Science 296, 1308–1313. [PubMed: 11964443]

Brembeck FH, Rosário M, and Birchmeier W (2006). Balancing cell adhesion and Wnt signaling, the key role of beta-catenin. Curr. Opin. Genet. Dev 16, 51–59. [PubMed: 16377174]

Brittle A, Thomas C, and Strutt D (2012). Planar polarity specification through asymmetric subcellular localization of Fat and Dachsous. Curr. Biol 22, 907–914. [PubMed: 22503504]

Campbell G, Weaver T, and Tomlinson A (1993). Axis specification in the developing Drosophila appendage: the role of wingless, decapentaplegic, and the homeobox gene aristaless. Cell 74, 1113–1123. [PubMed: 8104704]

Chen YT, Stewart DB, and Nelson WJ (1999). Coupling assembly of the E-cadherin/beta-catenin complex to efficient endoplasmic reticulum exit and basal-lateral membrane targeting of E-cadherin in polarized MDCK cells. J. Cell Biol 144, 687–699. [PubMed: 10037790]

Chen CL, Gajewski KM, Hamaratoglu F, Bossuyt W, Sansores-Garcia L, Tao C, and Halder G (2010). The apical-basal cell polarity determinant Crumbs regulates Hippo signaling in Drosophila. Proc. Natl. Acad. Sci. USA 107, 15810–15815. [PubMed: 20798049]

Chen YJ, Huang J, Huang L, Austin E, and Hong Y (2017). Phosphorylation potential of Drosophila E-Cadherin intracellular domain is essential for development and adherens junction biosynthetic dynamics regulation. Development 144, 1242–1248. [PubMed: 28219947]

Courjean O,Chevreux G,Perret E,Morel A,Sanglier S,Potier N,Engel J, van Dorsselaer A, and Feracci H (2008). Modulation of E-cadherin monomer folding by cooperative binding of calcium ions. Biochemistry 47, 2339–2349. [PubMed: 18232713]

Cui C, Merritt R, Fu L, and Pan Z (2017). Targeting calcium signaling in cancer therapy. Acta Pharm. Sin. B 7, 3–17. [PubMed: 28119804]

Curtis MW, Johnson KR, and Wheelock MJ (2008). E-cadherin/catenin complexes are formed cotranslationally in the endoplasmic reticulum/Golgi compartments. Cell Commun. Adhes 15, 365–378. [PubMed: 18937087]

Denmeade SR, Mhaka AM, Rosen DM, Brennen WN, Dalrymple S, Dach I, Olesen C, Gurel B, Demarzo AM, Wilding G, et al. (2012). Engineering a prostate-specific membrane antigen-activated tumor endothelial cell prodrug for cancer therapy. Sci. Transl. Med 4, 140ra86.

Eid JP, Arias AM, Robertson H, Hime GR, and Dziadek M (2008). The Drosophila STIM1 orthologue, dSTIM, has roles in cell fate specification and tissue patterning. BMC Dev. Biol 8, 104. [PubMed: 18950512]

Griffin JN, Del Viso F, Duncan AR, Robson A, Hwang W, Kulkarni S, Liu KJ, and Khokha MK (2018). RAPGEF5 regulates nuclear translocation of beta-catenin. Dev. Cell 44, 248–260.e4. [PubMed: 29290587]

Heijmans J, van Lidth de Jeude JF, Koo BK, Rosekrans SL, Wielenga MC, van de Wetering M, Ferrante M, Lee AS, Onderwater JJ, Paton JC, et al. (2013). ER stress causes rapid loss of intestinal epithelial stemness through activation of the unfolded protein response. Cell Rep 3, 1128–1139. [PubMed: 23545496]

Janody F, Lee JD, Jahren N, Hazelett DJ, Benlali A, Miura GI, Draskovic I, and Treisman JE (2004). A mosaic genetic screen reveals distinct roles for trithorax and polycomb group genes in Drosophila eye development. Genetics 166, 187–200. [PubMed: 15020417]

Jin X, Walker MA, Felsovalyi K, Vendome J, Bahna F, Mannepalli S, Cosmanescu F, Ahlsen G, Honig B, and Shapiro L (2012). Crystal structures of *Drosophila* N-cadherin ectodomain regions reveal a

widely used class of Ca^{2+}-free interdomain linkers. Proc. Natl. Acad. Sci. USA 109, E127–E134. [PubMed: 22171007]

Katoh M (2012). Function and cancer genomics of *FAT* family genes (review). Int. J. Oncol 41,1913–1918. [PubMed: 23076869]

Ke H, Feng Z, Liu M, Sun T, Dai J, Ma M, Liu LP, Ni JQ, and Pastor- Pareja JC (2018). Collagen secretion screening in *Drosophila* supports a common secretory machinery and multiple Rab requirements. J. Genet. Genomics 45, 299–313.

Kim SA, Tai CY, Mok LP, Mosser EA, and Schuman EM (2011). Calcium-dependent dynamics of cadherin interactions at cell-cell junctions. Proc. Natl. Acad. Sci. USA 108, 9857–9862. [PubMed: 21613566]

Koch AW, Pokutta S, Lustig A, and Engel J (1997). Calcium binding and homoassociation of E-cadherin domains. Biochemistry 36, 7697–7705. [PubMed: 9201910]

Krausova M, and Korinek V (2014). Wnt signaling in adult intestinal stem cells and cancer. Cell. Signal 26, 570–579. [PubMed: 24308963]

Lee AG, and East JM (2001). What the structure of a calcium pump tells us about its mechanism. Biochem. J 356, 665–683. [PubMed: 11389676]

Lee JD, and Treisman JE (2001). The role of Wingless signaling in establishing the anteroposterior and dorsoventral axes ofthe eye disc. Development 128, 1519–1529. [PubMed: 11290291]

Ling C, Zheng Y, Yin F, Yu J, Huang J, Hong Y, Wu S, and Pan D (2010). The apical transmembrane protein Crumbs functions as a tumor suppressor that regulates Hippo signaling by binding to Expanded. Proc. Natl. Acad. Sci. USA 107, 10532–10537. [PubMed: 20498073]

Linneweber GA, Winking M, and Fischbach KF (2015). The cell adhesion molecules Roughest, Hibris, Kin of irre and Sticks and stones are required for long range spacing ofthe Drosophila wing disc sensory sensilla. PLoS One 10, e0128490. [PubMed: 26053791]

Mao Y, Rauskolb C, Cho E, Hu WL, Hayter H, Minihan G, Katz FN, and Irvine KD (2006). Dachs: an unconventional myosin that functions downstream of Fat to regulate growth, affinity and gene expression in Drosophila. Development 133, 2539–2551. [PubMed: 16735478]

Neumann CJ, and Cohen SM (1997). Long-range action of Wingless organizes the dorsal-ventral axis of the Drosophila wing. Development 124, 871–880. [PubMed: 9043068]

Nolo R, Abbott LA, and Bellen HJ (2000). Senseless, a Zn finger transcription factor, is necessary and sufficient for sensory organ development in Drosophila. Cell 102, 349–362. [PubMed: 10975525]

Olson ER, Pancratov R, Chatterjee SS, Changkakoty B, Pervaiz Z, and DasGupta R (2011). Yan, an ETS-domain transcription factor, negatively modulates the Wingless pathway in the Drosophila eye. EMBO Rep 12, 1047–1054. [PubMed: 21869817]

Ou CY, Lin YF, Chen YJ, and Chien CT (2002). Distinct protein degradation mechanisms mediated by Cul1 and Cul3 controlling Ci stability in Drosophila eye development. Genes Dev 16, 2403–2414. [PubMed: 12231629]

Periz G, and Fortini ME (1999). $Ca(^{2+})$-ATPase function is required for intracellular trafficking of the Notch receptor in Drosophila. EMBO J 18, 5983–5993. [PubMed: 10545110]

Prakriya M, and Lewis RS (2015). Store-operated calcium channels. Physiol. Rev 95, 1383–1436. [PubMed: 26400989]

Prakriya M, Feske S, Gwack Y, Srikanth S, Rao A, and Hogan PG (2006). Orai1 is an essential pore subunit of the CRAC channel. Nature 443, 230–233. [PubMed: 16921383]

Riedel F, Gillingham AK, Rosa-Ferreira C, Galindo A, and Munro S (2016). An antibody toolkit for the study of membrane traffic in Drosophila melanogaster. Biol. Open 5, 987–992. [PubMed: 27256406]

Robinson BS, Huang J, Hong Y, and Moberg KH (2010). Crumbs regulates Salvador/Warts/Hippo signaling in Drosophila via the FERM-domain protein Expanded. Curr. Biol 20, 582–590. [PubMed: 20362445]

Rodrigues AB, Werner E, and Moses K (2005). Genetic and biochemical analysis of the role of Egfr in the morphogenetic furrow of the developing *Drosophila* eye. Development 132, 4697–4707. [PubMed: 16207755]

Roti G, Carlton A, Ross KN, Markstein M, Pajcini K, Su AH, Perrimon N, Pear WS, Kung AL, Blacklow SC, et al. (2013). Complementary genomic screens identify SERCA as a therapeutic target in NOTCH1 mutated cancer. Cancer Cell 23, 390–405. [PubMed: 23434461]

Ryoo HD, Domingos PM, Kang MJ, and Steller H (2007). Unfolded protein response in a *Drosophila* model for retinal degeneration. EMBO J 26, 242–252. [PubMed: 17170705]

Sadeqzadeh E, de Bock CE, and Thorne RF (2014). Sleeping giants: emerging roles for the fat cadherins in health and disease. Med. Res. Rev 34, 190–221. [PubMed: 23720094]

Sanson B, White P, and Vincent JP (1996). Uncoupling cadherin-based adhesion from Wingless signalling in Drosophila. Nature 383, 627–630. [PubMed: 8857539]

Sanyal S, Consoulas C, Kuromi H, Basole A, Mukai L, Kidokoro Y, Krishnan KS, and Ramaswami M (2005). Analysis of conditional paralytic mutants in *Drosophila* sarco-endoplasmic reticulum calcium ATPase reveals novel mechanisms for regulating membrane excitability. Genetics 169, 737–750. [PubMed: 15520268]

Sarpal R, Pellikka M, Patel RR, Hui FY, Godt D, and Tepass U (2012). Mutational analysis supports a core role for *Drosophila* α-catenin in adherens junction function. J. Cell Sci 125, 233–245. [PubMed: 22266901]

Savignac M, Simon M, Edir A, Guibbal L, and Hovnanian A (2014). SERCA2 dysfunction in Darier disease causes endoplasmic reticulum stress and impaired cell-to-cell adhesion strength: rescue by Miglustat. J. Invest. Dermatol 134, 1961–1970. [PubMed: 24390139]

Sehgal P, Szalai P, Olesen C, Praetorius HA, Nissen P, Christensen SB, Engedal N, and Møller JV (2017). Inhibition of the sarco/endoplasmic reticulum (ER) Ca^{2+}-ATPase by thapsigargin analogs induces cell death via ER Ca^{2+} depletion and the unfolded protein response. J. Biol. Chem 292, 19656–19673. [PubMed: 28972171]

Sharma P, and McNeill H (2013). Fat and Dachsous cadherins. Prog. Mol. Biol. Transl. Sci 116,215–235. [PubMed: 23481197]

Silva E, Tsatskis Y, Gardano L, Tapon N, and McNeill H (2006). The tumor-suppressor gene fat controls tissue growth upstream of expanded in the hippo signaling pathway. Curr. Biol 16, 2081–2089. [PubMed: 16996266]

Stamos JL, and Weis WI (2013). The β-catenin destruction complex. Cold Spring Harb. Perspect. Biol 5, a007898. [PubMed: 23169527]

Thastrup O, Cullen PJ, Drøbak BK, Hanley MR, and Dawson AP (1990). Thapsigargin, a tumor promoter, discharges intracellular Ca^{2}+ stores by specific inhibition of the endoplasmic reticulum $Ca^{2(+)}$-ATPase. Proc. Natl. Acad. Sci. USA 87, 2466–2470. [PubMed: 2138778]

Tsukasaki Y, Miyazaki N, Matsumoto A, Nagae S, Yonemura S, Tanoue T, Iwasaki K, and Takeichi M (2014). Giant cadherins Fat and Dachsous self-bend to organize properly spaced intercellular junctions. Proc. Natl. Acad. Sci. USA 111, 16011–16016. [PubMed: 25355906]

Uhl JD, Zandvakili A, and Gebelein B (2016). A Hox transcription factor collective binds a highly conserved Distal-less cis-regulatory module to generate robust transcriptional outcomes. PLoS Genet 12, e1005981. [PubMed: 27058369]

Vendome J, Posy S, Jin X, Bahna F, Ahlsen G, Shapiro L, and Honig B (2011). Molecular design principles underlying β-strand swapping in the adhesive dimerization of cadherins. Nat. Struct. Mol. Biol 18, 693–700. [PubMed: 21572446]

Venkiteswaran G, and Hasan G (2009). Intracellular Ca^{2+} signaling and store-operated Ca^{2+} entry are required in *Drosophila* neurons for flight. Proc. Natl. Acad. Sci. USA 106, 10326–10331. [PubMed: 19515818]

Walter P, and Ron D (2011). The unfolded protein response: from stress pathway to homeostatic regulation. Science 334, 1081–1086. [PubMed: 22116877]

Wehrli M, Dougan ST, Caldwell K, O'Keefe L, Schwartz S, Vaizel- Ohayon D, Schejter E, Tomlinson A, and DiNardo S (2000). *arrow* encodes an LDL-receptor-related protein essential for Wingless signalling. Nature 407, 527–530. [PubMed: 11029006]

Willecke M, Hamaratoglu F, Kango-Singh M, Udan R, Chen CL, Tao C, Zhang X, and Halder G (2006). The Fat cadherin acts through the Hippo tumor-suppressor pathway to regulate tissue size. Curr. Biol 16, 2090–2100. [PubMed: 16996265]

Williams JA, Bell JB, and Carroll SB (1991). Control of Drosophila wing and haltere development by the nuclear vestigial gene product. Genes Dev 5 (12B), 2481–2495. [PubMed: 1752439]

Wuytack F, Raeymaekers L, and Missiaen L (2002). Molecular physiology of the SERCA and SPCA pumps. Cell Calcium 32, 279–305. [PubMed: 12543090]

Yu FX, Zhao B, and Guan KL (2015). Hippo pathway in organ size control, tissue homeostasis, and cancer. Cell 163, 811–828. [PubMed: 26544935]

Zecca M, Basler K, and Struhl G (1996). Direct and long-range action of a Wingless morphogen gradient. Cell 87, 833–844. [PubMed: 8945511]

Zhang K, and Kaufman RJ (2006). The unfolded protein response: a stress signaling pathway critical for health and disease. Neurology 66 (2, Suppl 1), S102–S109. [PubMed: 16432136]

Zhu W, Leber B, and Andrews DW (2001). Cytoplasmic O-glycosylation prevents cell surface transport of E-cadherin during apoptosis. EMBO J 20, 5999–6007. [PubMed: 11689440]

Highlights

- Reduced activity of the ER calcium pump SERCA interferes with Wnt signaling
- β-catenin cannot signal when bound to E-cadherin that is retained in the ER
- Hippo and Notch signaling are only affected by a stronger reduction in ER calcium

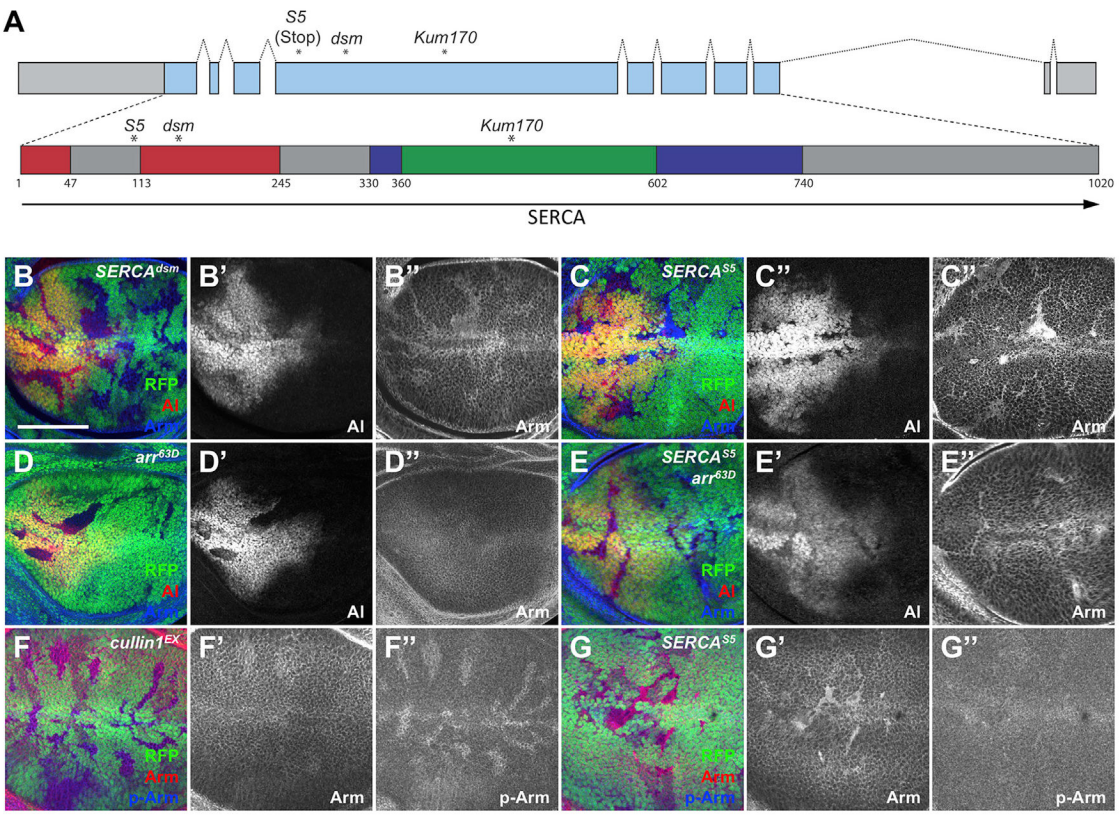

Figure 1. *SERCA* Mutations Affect Wg Signaling

(A) Diagram of the *SERCA* gene, showing the coding region in blue and the positions of the introns. Below is the encoded protein, showing the transmembrane domains (gray), actuator domain (red), phosphorylation domain (blue), and nucleotide-binding domain (green). Asterisks indicate the positions of the *dsm, S5*, and *Kum170* mutations.

(B-G) Third instar wing imaginal discs containing $SERCA^{dsm}$ (B), $SERCA^{S5}$ (C and G), arr^{63D} (D), arr^{63D}, $SERCA^{S5}$ (E), or $cul1^{EX}$ (F) clones marked by the absence of RFP (green). Anterior is to the left and dorsal up in this and all subsequent figures. Discs are stained with anti-Al (B'-E', red in B-E), anti-Arm (B"-E", F', and G'; blue in B-E, red in F and G), or anti-phospho-Arm (F" and G"; blue in F and G). Al levels decrease and unphosphorylated Arm accumulates in *SERCA* mutant clones. Arm also accumulates in arr^{63D}, $SERCA^{S5}$ double mutant clones, but not in arr^{63D} clones. Scale bar, 50 μm. n ≥ 10 discs for all stainings shown in this and all subsequent figures.

See also Figure S1.

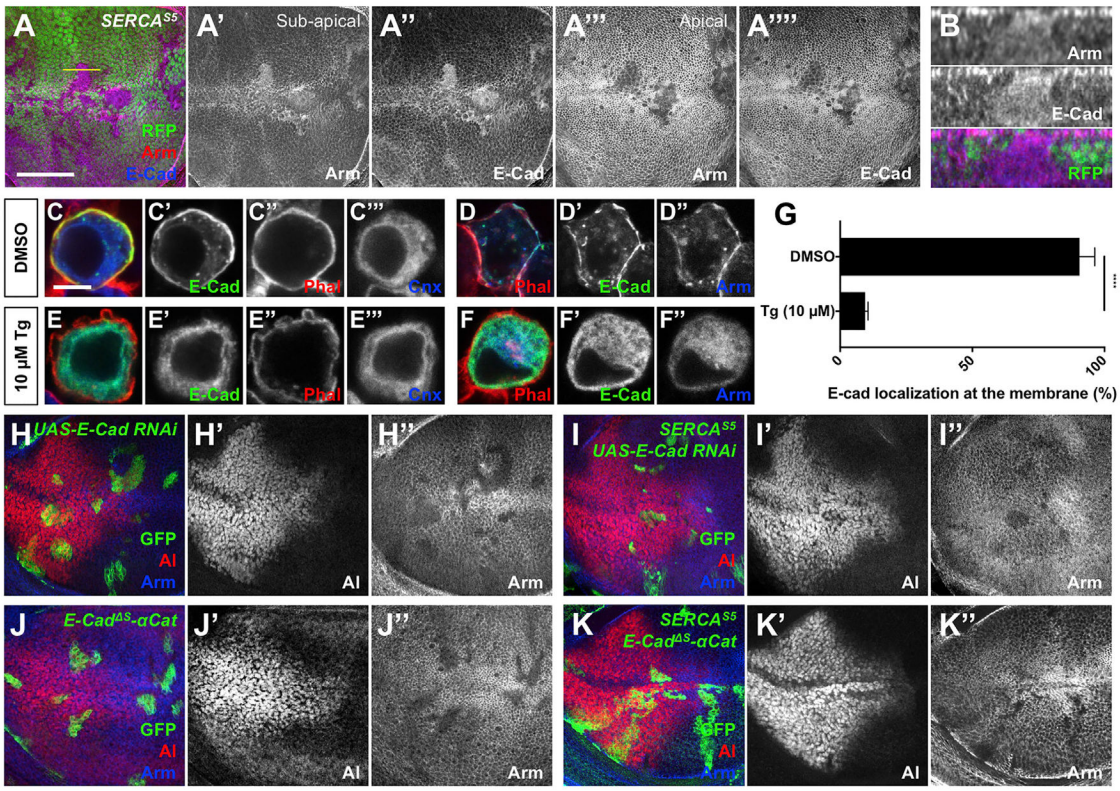

Figure 2. E-Cad Is Retained in the Endoplasmic Reticulum and Traps Arm There in the Absence of *SERCA*

(Aand B) Wing disc containing *SERCA*^{S5} clones marked bythe absence of RFP (green) stained with anti-Arm (A' and A"'; red in A) and anti-E-Cad (A" and A""; blue in A). Subapical sections are shown in A-A", and apical sections in A"' and A"". Scale bar, 50 μm. (B) z projection through the disc at the position shown by the line in (A), with apical up. In mutant cells, E-Cad colocalizes with Arm below the AJs.

(C-F) S2 cells co-transfected with *Act-GAL4* and *UAS-E-Cad* and treated with DMSO (C and D)or10 μM thapsigargin (Tg) (E and F) were stained with anti-E-Cad (C'-F'; green in C-F), phalloidin (C" and E"; red in C-F), anti-Cnx99A (C"' and E"'; blue in C and E), or anti-Arm (D" and F"; blue in D and F). Scale bar, 5 μM. (G) Quantification of the percentage of cells (means ± SEMs) in which E-Cad is localized at the plasma membrane in Tg- or DMSO-treated cells. ****p < 0.0001 by unpaired t test on three independent experiments. InTg-treated cells, E-Cad does not reach the plasma membrane and colocalizes with Cnx99A. Arm colocalizes with E-Cad in control and Tg-treated cells.

(H-K) Wing discs with wild-type (H) or *SERCA*^{S5} clones (I) expressing *E-Cad RNAi*, *E-Cad*$^{\Delta S\text{-}\alpha Cat}$ clones (J) or *SERCA*^{S5}, *E-Cad*$^{\Delta S\text{-}\alpha Cat}$ clones (K). Clones are positively marked with GFP (green) and stained with anti-Al (H'-K'; red in H-K) and anti-Arm (H"-K"; blue in H-K). *E-Cad*$^{\Delta S\text{-}\alpha Cat}$ rescuesArm accumulation and *al* expression in *SERCA*^{S5} clones. See also Figure S2.

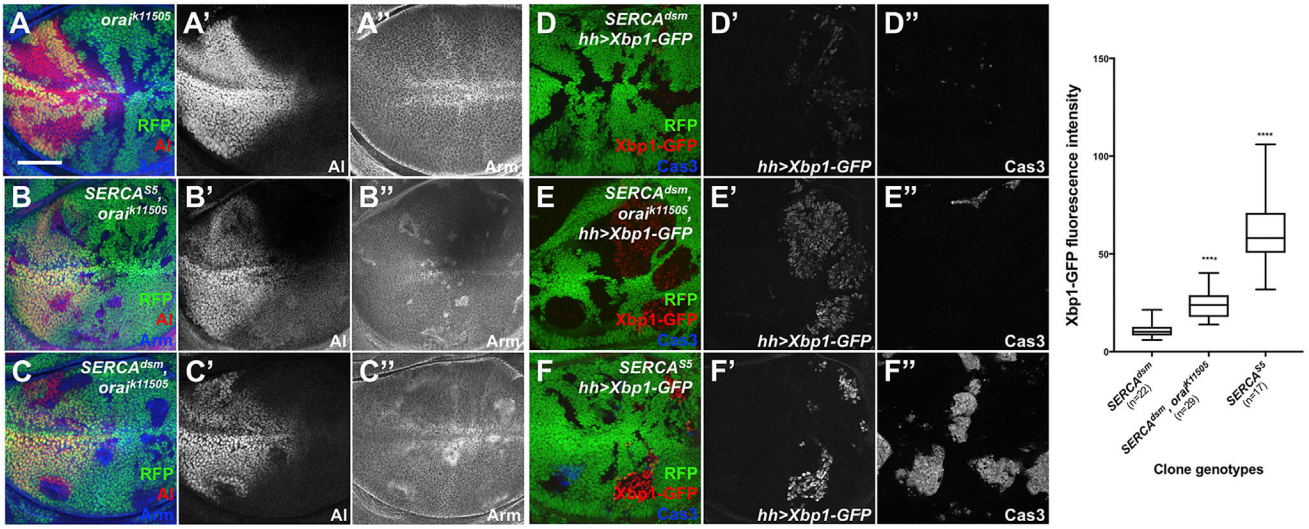

Figure 3. Three Levels of ER Stress Induced by *SERCA* and *orai* Mutations

(A-F) Wing discs with *orai*^{k11505} (A), *SERCA*^{S5}*, orai*^{k11505} (B), *SERCA*^{dsm}*, orat*^{11505} (Cand E), *SERCA*^{dsm} (D), or *SERCA*^{S5} (F)clones labeled bytheabsence ofRFP (green). (A-C) Discs are stained with anti-Al (A'-C'; red in A-C) and anti-Arm (A"-C"; blue in A-C). Scale bar, 50 μm. Disrupting Orai channel function does not rescue *SERCA* mutants. (D-F) The endoplasmic reticulum (ER) stress reporter *Xbp-1-GFP* (D'-F'; red in D-F) is driven in the posterior compartment with *hh-Gal4*. Discs are also stained with anti-activated caspase 3 (basal sections shown in D"-F"; blue in D-F). Loss of *orai* increases ER stress in *SERCA*^{dsm} cells, but not to the level seen in *SERCA*^{S5} cells, which induces apoptosis. (G) Quantification ofXbp1-GFP intensity in *SERCA*^{dsm}*; SERCA*^{dsm}*, orai*^{k11505}; and *SERCA*^{S5} clones. Box-and-whisker plot shows median bounded by minimum, first quartile, third quartile, and maximum. *SERCA*^{dsm}, n = 22 clones in 5 wing discs; *SERCA*^{dsm}*, orai*^{k1505} n = 22 clones in 6 discs; *SERCA*^{S5} n = 29 clones in 7 discs; ****p < 0.0001 by Welch's ANOVA.

See also Figure S3.

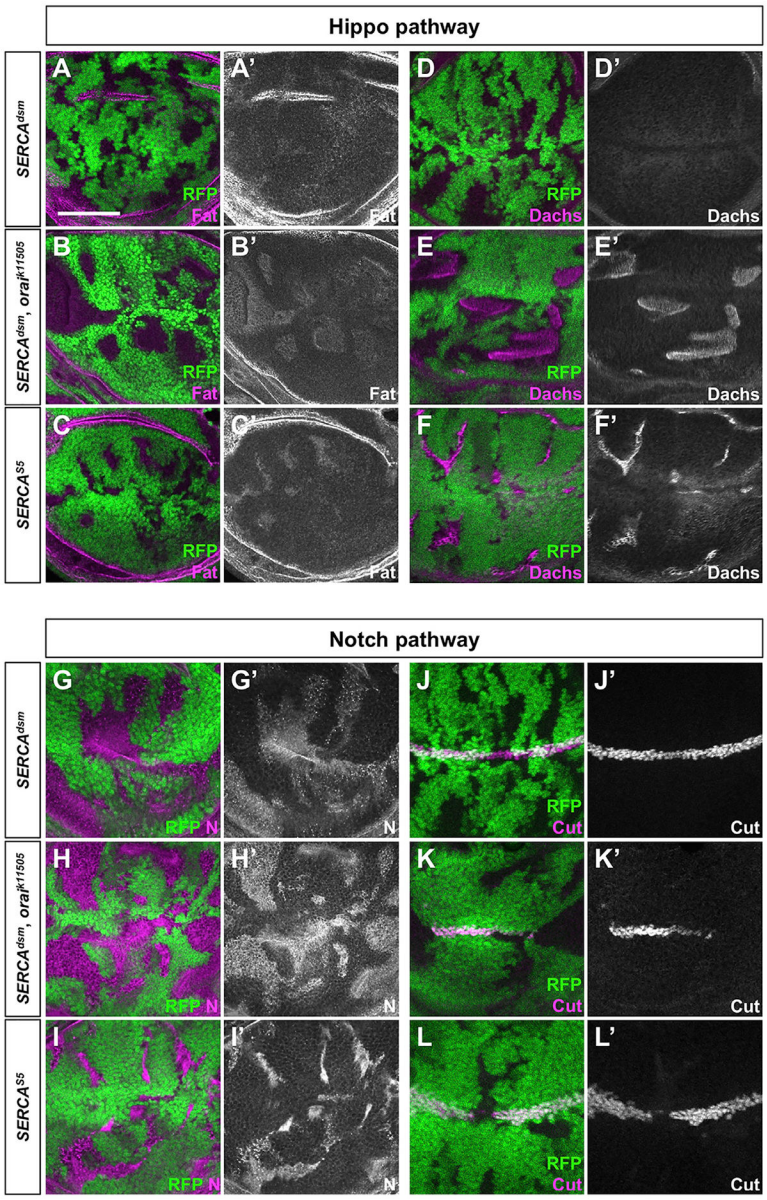

Figure 4. Hippo and Notch Signaling Pathways Are Affected by Moderate ER Stress

(A-L) Wing imaginal discs with *SERCA*^{dsm} (A, D, G, and J), *SERCA*^{dsm}, *orai*^{k11505} (B, E, H, and K), or *SERCA*^{S5} clones (C, F, I, and L), marked by the absence of RFP (green) and stained with antibodies to Fat (A'-C'; magenta in A-C), Dachs (D'-F'; magenta in D-F), Notch (G'-I'; magenta in G-I), or Cut (J'-L'; magenta in J-L). Scale bar, 50 mm. Subapical sections are shown, except in (D)-(F), which show the apical membrane. Although there is a weak subapical accumulation of Fat and Notch in *SERCA*^{dsm} clones, Dachs and Cut are not affected. Decreasing levels of ER Ca^{2}+ in *SERCA*^{dsm}, *orai*^{k11505} and *SERCA*^{S5} clones cause an increasing accumulation of Fat and Notch, leading to the membrane localization of Dachs and loss of Cut.

See also Figure S4.

KEY RESOURCES TABLE

REAGENT or RESOURCE	SOURCE	IDENTIFIER
Antibodies		
Rat polyclonal anti-Aristaless	Campbell et al., 1993	N/A
Chicken polyclonal anti-GFP	Invitrogen	Cat# A10262
Mouse monoclonal anti-Armadillo	Developmental Studies Hybridoma Bank	Cat # N2 7A1; RRID AB_528089
Rabbit polyclonal anti-phospho-β-catenin (Ser45)	Cell Signaling	Cat # 9564; RRID AB_331150
Rat monoclonal anti-E-cadherin	Developmental Studies Hybridoma Bank	Cat # DCAD2; RRID AB_528120
Rabbit polyclonal anti-active caspase 3	BD PharMingen	Cat # 559565
Mouse monoclonal anti-Notch	Developmental Studies Hybridoma Bank	Cat # C17.9C6; RRID AB_528410
Mouse monoclonal anti-Cut	Developmental Studies Hybridoma Bank	Cat # 2B10; RRID AB_528186
Mouse monoclonal anti-Cnx99A	Developmental Studies Hybridoma Bank	Cat # Cnx99A 6-2-1; RRID AB_2722011
Mouse monoclonal anti-Achaete	Developmental Studies Hybridoma Bank	Cat # anti-achaete; RRID AB_528066
Mouse monoclonal anti-Frizzled2	Developmental Studies Hybridoma Bank	Cat # 1A3G4; RRID AB_528257
Mouse monoclonal anti-Crumbs	Developmental Studies Hybridoma Bank	Cat # Cq4; RRID AB_528181
Rabbit polyclonal anti-Fat	Brittle et al., 2012	N/A
Rabbit polyclonal anti-Dachs	Brittle et al., 2012	N/A
Rat polyclonal anti-Distal-less	Uhl etal., 2016	N/A
Rabbit polyclonal anti-Vestigial	Williams et al., 1991	N/A
Guinea pig polyclonal anti-Senseless	Nolo et al., 2000	N/A
Rabbit polyclonal anti-Epidermal Growth Factor Receptor	Rodrigues et al., 2005	N/A
Rabbit polyclonal anti-Hibris	Linneweber et al., 2015	N/A
Alexa Fluor 555-conjugated phalloidin	Invitrogen	Cat # A34055
Chemicals, Peptides, and Recombinant Proteins		
Effectene Transfection Reagent	QIAGEN	Cat # 301425
Tg	Santa Cruz Biotechnology	Cat # sc-24017
GIBCO® Schneider's *Drosophila* medium	Invitrogen	Cat #21720001
GIBCO® Fetal bovine serum, qualified, heat inactivated	Invitrogen	Cat# 16140–071
Experimental Models: Cell Lines		
D. melanogaster: Cell line S2: S2-DRSC	Laboratory of Ruth Lehmann	FlyBase: FBtc0000181
Experimental Models: Organisms/Strains		

REAGENT or RESOURCE	SOURCE	IDENTIFIER
D. melanogaster: SERCA^{dsm}	This paper	N/A
D. melanogaster: SERCA^{kum170}	Sanyal et al., 2005	Flybase: FBal0184441
D. melanogaster: SERCA^{S5}	Periz and Fortini, 1999	Flybase: FBal0101766
D. melanogaster: orai^{k11505}	Bloomington *Drosophila* Stock Center	BDSC:11042; Flybase: FBst0011042
D. melanogaster: arr^{630}	Janody et al., 2004	Flybase: FBal0155633
D. melanogaster: fz3-RFP	Olson et al., 2011	Flybase: FBtp0071231
D. melanogaster: E-Cad$^{\Delta S\text{-}\alpha Cat}$-GFP	Chen et al., 2017	N/A
D. melanogaster: E-Cad$^{\Delta \beta S\text{-}\alpha Cat}$-GFP	Chen et al., 2017	N/A
D. melanogaster: UAS-Xbp1-GFP	Ryoo et al., 2007	Flybase: FBal0230351
D. melanogaster: UAS-Ecad RNAi y^{1} sc* v^{1}; P{TRiP.HMS00693}attP2	Bloomington *Drosophila* Stock Center	BDSC:32904; Flybase: FBst0032904
D. melanogaster: UAS-Stim RNAi w*; P{UAS-Stim.RNAi.E}26–1	Bloomington *Drosophila* Stock Center	BDSC:41758; Flybase: FBst0041758
D. melanogaster: FRT42, cul1^{EX}	Ou et al., 2002	Flybase: FBal0141058
D. melanogaster: FRT82, axn^{E77}	Lee and Treisman, 2001	Flybase: FBal0121005
D. melanogaster: Ubx-FLP	Bloomington *Drosophila* Stock Center	FlyBase: FBti0150334
D. melanogaster: hh-GAL4	Bloomington *Drosophila* Stock Center	FlyBase: FBti0017278
D. melanogaster: Df(2R)BSC601	Bloomington *Drosophila* Stock Center	FlyBase: FBab0045520
D. melanogaster: Df(2R)BSC770	Bloomington *Drosophila* Stock Center	FlyBase: FBab0045836
Recombinant DNA		
pActin-GAL4 plasmid	Laboratory of Nathalie Dostatni	Flybase: FBal0097155
pUAS-Ecad plasmid	Sarpal et al., 2012	N/A
Software and Algorithms		
ImageJ 1.50d	National Institutes of Health	https://imagej.nih.gov/ij/ https://imagej.nih.gov/ij/.
GraphPad Prism 7.0c	GraphPad Software, Inc.	https://www.graphpad.com